ISSN: 0128-7680
Pertanika J. Sci. & Technol. **20 (1)**: 81 – 88 (2012)

Effect of Rare Earth Elements Substitution in La site for $LaMnO_3$ Manganites

Wong Jen Kuen*, Lim Kean Pah, Abdul Halim Shaari, Chen Soo Kien, Ng Siau Wei and Albert Gan Han Ming
Department of Physics, Faculty of Science, Universiti Putra Malaysia, 43400 Serdang, Selangor, Malaysia
**E-mail: wjenkuen@hotmail.com*

ABSTRACT

With a view to understanding the effect of rare earth element (Ce, Pr, Nd, Sm and Gd) substitution for the La site in $LaMnO_3$ (LMO), the samples were prepared via solid-state reaction. Structure investigation by X-ray diffraction (XRD) showed that structure transformation from trigonal (LMO) to orthorhombic (PMO, NMO, SMO and GMO) occurred when smaller trivalent rare earth element was replaced. The MnO_6 octahedra were tilted and elongated or compressed, corresponding to the ionic radii of the rare earth inserted. Meanwhile, microstructure study using scanning electron microscopy (SEM) illustrated that La substitution by another rare earth element caused a reduction in grain size. This might due to the changes in enthalpy of fusion by other rare earth ions, where higher enthalpy of fusion favours formation of smaller grain size. However, $CeMnO_3$ did not form under this preparation condition. The magnetic properties studied from the hysteresis plot taken at room temperature indicated that the substitution of La with other magnetic trivalent rare earth ions strongly weakened the magnetic strength of the system.

Keywords: Magnetic Material, Manganite Perovskite, Rare-earth ions, Rietveld refinement, Structure Transformation

INTRODUCTION

$LnMnO_3$ (Ln = rare earth element) has a perovskite-type structure for Ln = La to Dy. This particular compound and its solid solutions, with alkaline earth elements, have been extensively studied because of their potential applications in magnetic insulation and for Colossal Magnetoresistance (CMR) (Kobayashi *et al*., 2008; Mahesh *et al*., 1995). $LaMnO_3$, which is also known as Mott Insulator (Yasuo, 2004), has A-type magnetic order, in which the spins are ferromagnetically aligned in planes while anti-ferromagnetically when aligned between the planes (Murakami *et al*., 1998). The replacement of non-magnetic La^{3+} with a magnetic ion would either increase or decrease the net magnetization value, M_s. This value is expressed as $M_s = M_{Mn} + M_A$, where M_{Mn} and M_A are the magnetizations of Mn and the 'A' site sub-lattice, respectively (Song *et al*., 2008). Meanwhile, the crystal structure of $LnMnO_3$ consists of Mn ion surrounded by oxygen atoms forming the MnO_6 octahedra when different types of Ln site cations are located between them (Van Tendeloo *et al*., 2004). From a previous study, the crystal structure of $LaMnO_3$ was found to vary from orthorhombic (*Pbnm*) to rhombohedral (*R-3c*), depending on the method of synthesis (Töpfer *et al*., 1997) with the lattice parameters of $a = b = 5.523$Å and $c = 13.324$Å (Moreno *et al*., 2008) as well as the oxygen stoichiometry of $LnMnO_{3-\delta}$ (Ln= La, Pr, Nd, Sm and Y) (Atsumi *et al*., 1997). In this work, the

Received: 11 August 2010
Accepted: 20 December 2010
*Corresponding Author

influence of the structure changes, microstructure and room temperature magnetism induced by the substitution of different trivalent rare earth ions in the La site for $LaMnO_3$ was studied since each trivalent rare earth ion possessed its own unique behaviour. The ionic radii of La^{3+}, Ce^{3+}, Pr^{3+}, Nd^{3+}, Sm^{3+}, and Gd^{3+} were 1.172 Å, 1.150 Å, 1.130 Å, 1.123 Å, 1.098 Å and 1.078 Å, respectively (Aspinall *et al*., 2001).

MATERIALS AND METHODS

Polycrystalline pellets $AMnO_3$ (A= La, Ce, Pr, Nd, Sm and Gd) were fabricated using a solid-state reaction method. Stoichiometric amounts of the starting powders (La_2O_3, CeO_2, Pr_6O_{11}, Nd_2O_3, Sm_2O_3, Gd_2O_3 and $MnCO_3$), with the purity ≥ 99.9%, were mixed and wet-milled in acetone. The homogeneous mixture was dried at 100°C and ground before calcination (900°C for 12 hours). The samples were reground and sieved using a 38 µm sized sieve. The sieved powders were pressed into pellets and sintered at 1300°C for 24 hours. They formed $LaMnO_3$ (LMO), $CeMnO_3$ (CMO), $PrMnO_3$ (PMO), $NdMnO_3$ (NMO), $SmMnO_3$ (SMO) and $GdMnO_3$ (GMO). The microstructure and structure of the samples were then characterized using the scanning electron microscopy (SEM, LEO1455 VPSEM, with an OXFORD INCA ENERGY 300EDX attachment) and X-ray diffraction (XRD, Phillips PW 3040/60 Xpert Pro). The XRD data were collected using a continuous scan with the step size of 0.033° in gonio scan axis. The data were analyzed using Rietveld refinement with X'Pert HighsScore Plus programme. The magnetic properties of the samples were measured at room temperature using a vibrating sample magnetometer (VSM, LakeShore Model 7407).

RESULTS AND DISCUSSION

The SEM micrographs shown in *Fig. 1* illustrate that all the grains are well connected and in a single phase, except for the two different microstructures shown in CMO. There is a significant contrast among the grains of CMO which are separated into lighter and darker colours. This was confirmed by EDX, i.e. lighter grains contained higher amount of Ce ion while darker grains consisted of more Mn ions. The grain sizes of LMO, CMO (mixture of CeO_2 and Mn_3O_4), PMO, NMO, SMO, and GMO were found to be in the range of 7.1~9.3 µm, CMO (light grains = 1.6~5.2 µm, darker grains = 0.9~3.0 µm), 2.1~5.0 µm, 0.6~4.3 µm, 1.0~3.0 µm and 0.5~2.1 µm, respectively. It was found that the decrease in the grain size and the range of sizes were mainly due to the change in the enthalpy of fusion of different rare earth ions. As the enthalpy of fusion of La^{3+}, Ce^{3+}, Pr^{3+}, Nd^{3+}, Sm^{3+}, and Gd^{3+} were 6.2, 5.46, 6.89, 7.14, 8.62, and 10.05 kJ/mole, respectively (Barbalace, 2010), the formation of grain size decreases when the enthalpy of fusion of substituted ion increases. However, two different types of microstructure were observed in the CMO sample, and these correspond with cerium oxide and manganese oxide (confirmed via EDX). Manganese oxide is a decomposed product from manganese carbonate. Ce has the smallest value of enthalpy of fusion among the rare earth ions and due to its highly thermal stability, cerium oxide does not react with manganese oxide to form $CeMnO_3$ (CMO).

Structure investigations were carried out using a Philips X-ray diffractometer with CuK_α radiation in 2θ range of 20-80°. The data for each sample were matched, refined and plotted. The matched XRD patterns of all the samples are single phase, with the exception of CMO. From the XRD database, the material obtained was the reaction with cerium oxide which gave a spectrum that matched a combination of the CeO_2 and Mn_3O_4 standards. This further confirmed the existence of two oxides and verified that the desired CMO was not formed using the method proposed in this work.

From the Rietveld refinement analysis with the ICSD (Inorganic Crystal Structure Database) crystallographic database, the unit cell parameters and other fitting parameters are summarized in

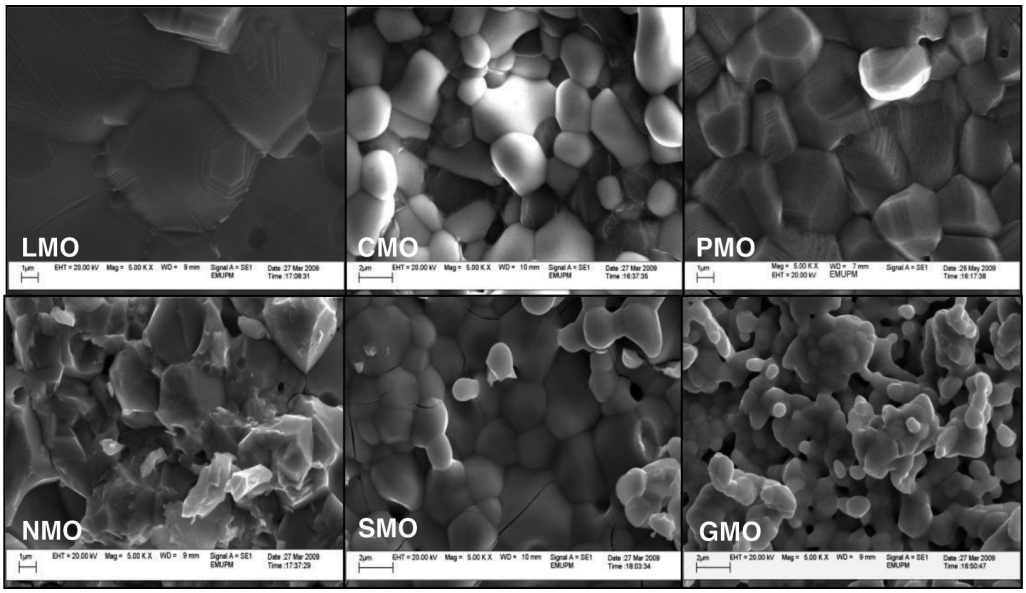

Fig. 1: SEM micrographs (5000X) of $AMnO_3$ (A= La, Ce, Pr, Nd, Sm and Gd)

Tables 1 and 2. As observed, the crystal structure changed from trigonal (LMO) to orthorhombic (PMO, NMO, SMO, and GMO). Overall, the unit cell parameters *a*, *b* and *c* decreased as smaller trivalent rare earth cation was substituted in the La site. This was probably due to the fact that the substitution of smaller ions in the La site shrunk the overall unit cell. As reported earlier, LMO was expected to be in orthorhombically distorted perovskite structure (Atsumi *et al*., 1997), but in this work, LMO was found to have a trigonal crystal structure. This might due to the lack of oxygen or dissociation similar to that reported by Atsumi *et al*. (1996).

The changes in both bond length and bond angle of Mn-O-Mn long range order resulted from MnO_6 octahedral were observed. Detailed studies on crystal structures are given in Table 2. Oxygen

TABLE 1
Crystallographic data of perovskite manganites

Sample code	LMO	PMO	NMO	SMO	GMO
Chemical formula	$LaMnO_3$	$PrMnO_3$	$NdMnO_3$	$SmMnO_3$	$GdMnO_3$
Crystal System	Trigonal	Orthorhombic	Orthorhombic	Orthorhombic	Orthorhombic
Space Group	*R -3 c*	*Pnma*	*Pnma*	*Pnma*	*Pnma*
Lattice parameter					
a (Å)	5.5320 (2)	5.7970 (1)	5.7920 (1)	5.8412 (1)	5.8511 (2)
b (Å)	5.5320 (2)	7.5892 (1)	7.5640 (1)	7.4838 (1)	7.4432 (3)
c (Å)	13.3664 (7)	5.4496 (1)	5.4216 (7)	5.35866 (9)	5.3154 (2)
Volume of cell ($Å^3$)	354.2529	239.7509	237.5216	234.251	231.4904
$R_{expected}$ (%)	4.5611	6.5695	3.6317	5.3531	2.7180
$R_{profile}$ (%)	8.1053	7.4170	9.4630	4.6500	3.1890
$R_{weighed\ profile}$ (%)	12.7308	9.6333	3.4608	5.9021	4.3941
Goodness of fit	8.4306	2.1501	3.7374	1.2156	2.6135

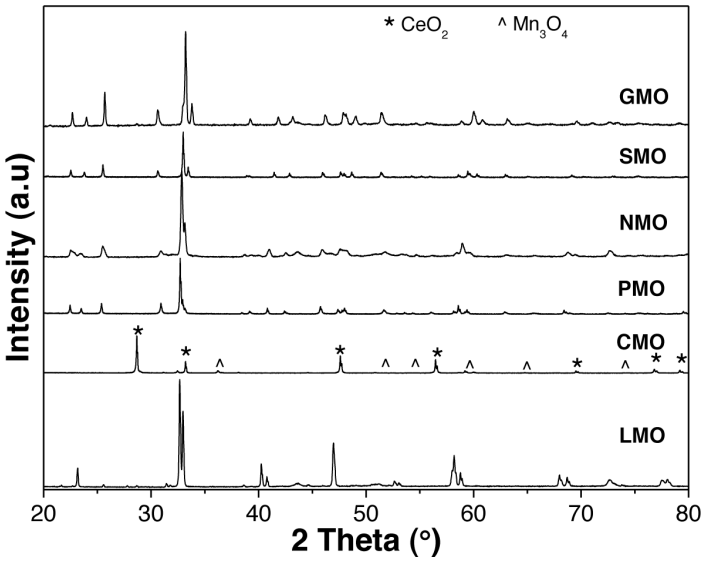

Fig. 2: X-ray diffraction pattern of Mn-based samples

atoms were found to be of different coordination which are classified as O(1) and O(2). However, this is not the case for LMO, since its crystal structure is trigonal and highly symmetric. Table 2 gives two different bond lengths between O(1) and Mn in the PMO, NMO, SMO and GMO samples. However, the Mn-O(2) bond length remains almost the same. On the other hand, the average bond angle of both Mn-O(1)-Mn and Mn-O(2)-Mn decreased as smaller ionic radii rare earth ions were substituted into the lattices. This was probably influenced by the diameter of the rare earth atoms which were located between MnO_6 octahedra. When MnO_6 was combined with rare earth elements of different ionic radii, it tended to deform to achieve a more stable shape. However, smaller ionic radii substitution not only drives MnO_6 octahedra to display tilting, but elongation and compression as well. This occurs mainly due to attractive forces from the neighbouring MnO_6 octahedra and at the same time, repulsion force was created to oppose that attraction force. Hence, the dimensions (bond length, Mn-O and Mn-O-Mn, bond angle) of MnO_6 as discussed would be altered (Van Tendeloo *et al*., 2004).

TABLE 2
Interatomic distance and bond angle of MnO_6 in $AMnO_3$ (A = La, Ce, Pr, Nd, Sm and Gd)

Sample code	LMO	PMO	NMO	SMO	GMO
Chemical formula	$LaMnO_3$	$PrMnO_3$	$NdMnO_3$	$SmMnO_3$	$GdMnO_3$
∠ Mn-O(1)-Mn (°)	165.780 (3)	151.658 (6)	154.380 (6)	146.854 (5)	150.090 (1)
∠ Mn-O(2)-Mn(°)		152.340 (8)	148.200 (6)	147.621 (6)	144.080 (1)
Mn-O(1) (Å)	1.962 × 6	1.916 × 2	1.941 × 2	1.909 × 2	1.852 × 2
		2.186 × 2	2.127 × 2	2.226 × 2	2.238 × 2
Mn-O(2) (Å)		1.954 × 2	1.966 × 2	1.948 × 2	1.956 × 2

From *Fig. 3*(a), the hysteresis loops of all the samples show a straight line crossing the origin, indicating either a paramagnetic or an anti-ferromagnetic behaviour. As depicted in Figure 3(b), however, drastic changes in magnetization values corresponding to the substituted magnetic trivalent rare earth ions at room temperature were clearly observed. The magnetization value of LMO is relatively much larger (~8 emu/g) compared to the other samples (<1 emu/g). Meanwhile, the magnetization value of each sample measured at 10 kG applied magnetic field decreased as magnetic trivalent rare earth ions (Ce, Pr, Nd, Sm and Gd) were substituted. This was probably due to the

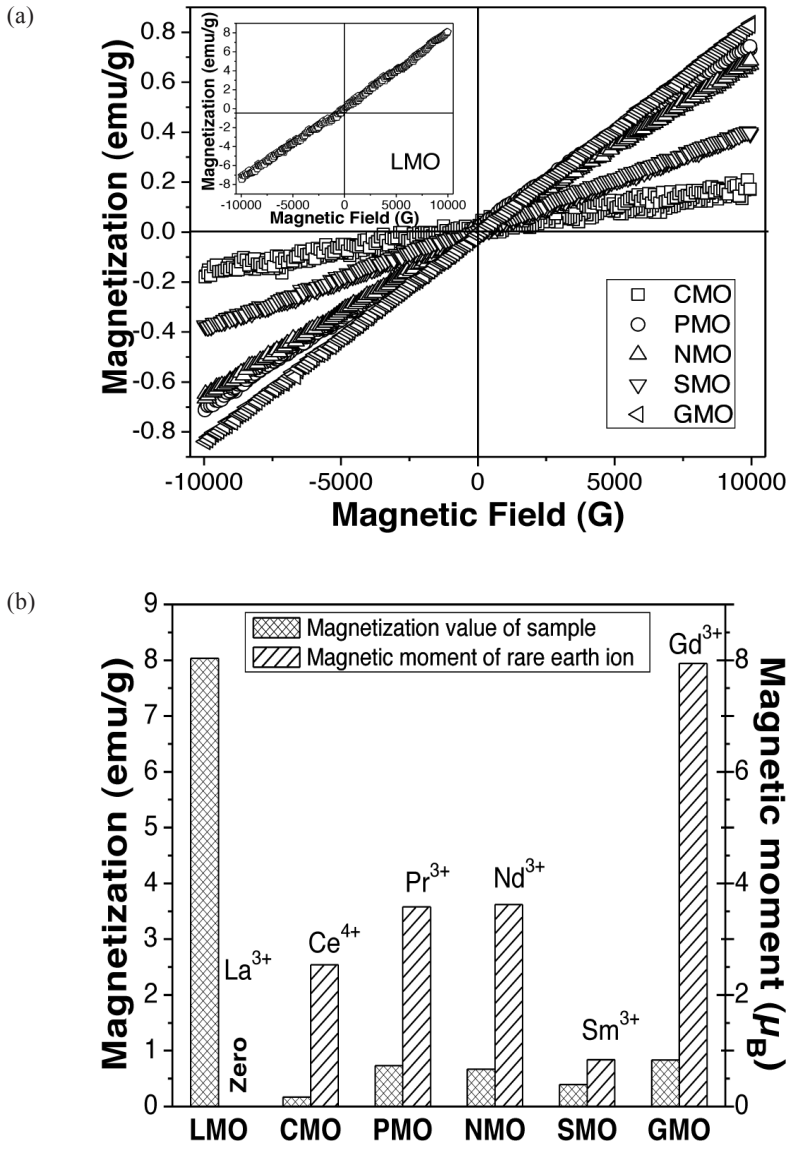

Fig. 3: (a) Hysteresis loops of $AMnO_3$ (A= La, Ce, Pr, Nd, Sm and Gd) (b) Magnetization value of the samples substituted by various rare earth ions at 10kG and magnetic moment of rare earth ions (Aspinall et al., 2001)

spins in the Mn sub-lattice which were pinned by the spins in the 'A' site sub-lattice. When an external magnetic field was applied, the pinned spins were unable to align with the direction of the applied magnetic field, and this subsequently decreased the net magnetization values. Since La^{3+} is a non-magnetic ion, it is reasonable that LMO exhibits the highest magnetization value, while CMO, PMO, NMO, SMO and GMO are smaller.

CONCLUSIONS

It was found that the substitution of Ce, Pr, Nd, Sm and Gd for La site in $LaMnO_3$ perovskite manganites greatly influenced their structures, especially the trivalent rare earth ions with small ionic radius. MnO_6 can be invoked to deform and doing this stabilizes the systems. Nonetheless, $CeMnO_3$ was not formed, but there were two different CeO_2 and Mn_3O_4 phases. The microstructure changed corresponding to the enthalpy of fusion of the substituted rare earth ion. Smaller enthalpy of fusion would lead to greater grain size. As observed in $LaMnO_3$, the substitution of La with other magnetic trivalent rare earth weakened their magnetic strength.

ACKNOWLEDGEMENT

The authors gratefully acknowledge the support from the Ministry of Science, Technology and Innovation of Malaysia (MOSTI) for the grant under the Fundamental Research Grant Scheme (FRGS) 01-11-09-728FR, Research University Grant Scheme (RUGS) 91849 and the award of the National Science Fellowship (NSF).

REFERENCES

Aspinall, H. C. (2001). *Chemistry of the f-block Elements (Advanced chemistry texts; v. 5) 10-18*. United Kingdom: Gordon and Breach Science Publishers.

Atsumi, T., Ohgushi, T., & Kamegashira, N. (1996). Studies on oxygen dissociation pressure of $LnMnO_3$ (Ln = rare earth) with the e.m.f. technique. *Journal of Alloys and Compounds, 238*(1-2), 35-40.

Atsumi, T., Ohgushi, T., Namikata, H., & Kamegashira, N. (1997). Oxygen nonstoichiometry of $LnMnO_{3-\delta}$ (Ln=La, Pr, Nd, Sm and Y). *Journal of Alloys and Compounds, 252*(1-2), 67-70.

Barbalace, K. (2010). Periodic Table of Elements. Retrieved on September 8, 2010 from EnvironmentalChemistry.com. http://EnvironmentalChemistry.com/yogi/periodic/.

Kobayashi, M., Tamura, H., Nakano, H., Satoh, H., & Kamegashira, N. (2008). Stability of phases in (Ba, Gd) MnO_3 solid solution system. *Journal of Rare Earths, 26*(2), 233-236.

Mahesh, R., Mahendiran, R., Raychaudhuri, A. K., & Rao C. N. R. (1995). Effect of the internal pressure due to the A-site cations on the giant magnetoresistance and related properties of doped rare earth manganites $Ln_{1-X}A_XMnO_3$ (Ln=La, Nd, Gd, Y; A=Ca, Sr, Ba, Pb). *Journal of Solid State Chemistry 120*, 160.

Moreno, L. C., Valencia, J. S., Landínez Téllez, D. A., Arbey Rodríguez M, J., Martínez, M. L., Roa-Rojas, J., & Fajardo, F. (2008). Preparation and structural study of $LaMnO_3$ magnetic material. *Journal of Magnetism and Magnetic Materials, 320*(14), e19-e21.

Murakami, Y., Hill, J.P., Gibbs, D., Blume, M., Koyama, I., Tanaka, M., Kawata, H., Arima, T., Tokura, Y., Hirota, K., & Endoh, Y. (1998). Resonant X-Ray Scattering from Orbital Ordering in $LaMnO_3$. *Physical Review Letter, 81*, 582-585.

Song, Q. X., Wang, G. Y., Yan, G. Q., Mao, Q., Wang, W. Q., & Peng, Z. S. (2008). Influence of substitution of Sm, Gd, and Dy for La in $La_{0.7}Sr_{0.3}MnO_3$ on its magnetic and electric properties and strengthening effect on room-temperature CMR. *Journal of Rare Earths*, 26(6), 821-826.

Töpfer, J., & Goodenough, J. B. (1997). $LaMnO_{3+\delta}$ Revisited. *Journal of Solid State Chemistry, 130*(1), 117-128.

Van Tendeloo, G., Lebedev, O. I., Hervieu, M., & Raveau, B. (2004). Structure and microstructure of colossal magnetoresistant materials. *Report on Progress in Physics, 67*, 1315-1365.

Yasuo, E. (2004). New scaling of spin excitations in ferromagnetic metals. *Physica B: Condensed Matter*, *345*, 132-136.